STScI | SPACE TELESCOPE SCIENCE INSTITUTE

Instrument Science Report COS 2025-05(v1)

COS/FUV Lifetime Position 5 Target Placement

Elaine M. Frazer[1], Kate Rowlands [1,2], Serge Dieterich[1], Travis Fischer[1,2], Rachel Plesha[1], David Sahnow[1]

[1] Space Telescope Science Institute, Baltimore, MD
[2] AURA for ESA, Space Telescope Science Institute, Baltimore, MD

1 April 2025

ABSTRACT

We report on the observations and analysis completed to find the optimal placement that centered the target in the fixed lifetime position (LP) 5 aperture of the Cosmic Origins Spectrograph (COS). In November 2020, we executed Program 16430, in which observations of the target star WD0947+857 were taken over a single two-orbit visit. During this visit, the target position was scanned across the fixed aperture in both the dispersion and cross-dispersion directions. By analyzing the throughputs at each position in comparison to the measured maximum, we calculated median offsets of -0.06690 arcseconds for the V2 coordinate and -0.00266 arcseconds for the V3 coordinate. These values were used to fine-tune the entries in the Science Instrument Aperture File (SIAF) that holds the locations of all COS apertures in spacecraft (V2, V3) coordinates at every LP. The SIAF was successfully updated in February 2021 for use with all LP5 calibration and science observations starting in Cycle 29.

Contents

1. Introduction 2
2. Program Design 2
3. Calibration 3

4. Analysis 6
5. Final SIAF Adjustments 8
6. Summary 8
Change History for COS ISR 2025-05 11
References 12

1. Introduction

As a part of the enabling phase for each lifetime position (LP) move on the Cosmic Origins Spectrograph's (COS) far ultraviolet (FUV) detector, we must update the Science Instrument Aperture File (SIAF), which contains the locations of the spectra for optimal target throughput. This file contains entries for both the primary science aperture (PSA) and bright object aperture (BOA) locations when in use (LFBOA* and LFPSA*, respectively, where the * stands for the appropriate LP character), as well as location of the BOA when the PSA is in use (LAPTFBOAF*), and the PSA when the BOA is in use (LAPTFPSAF*) for all COS LPs.

To find the optimal entries for the SIAF, we employ a multi-step process. Initially, an approximate position for the spectrum on the detector at the new LP is selected based on analysis done in the exploratory phase (James et. al., 2023), an aperture block position is selected, and the SIAF is updated with these entries. Then, data are obtained and analyzed to refine the target position, and the results are used to update the SIAF again. This process ensures that spectra from a source taken at this LP are well-centered in the aperture so that the calibration phase can commence. In this instrument science report, we detail the observations, analysis, and final adjustments made to the SIAF for COS's move to LP5, which placed all G130M cenwave 1291–1327 spectra at LP5 from LP4 and went into affect in October 2021 at the start of Cycle 29. More information about the LP5 enabling activities and motivation for moving to LP5 may be found in Sankrit et. al., 2023.

2. Program Design

The LP5 enabling program "Verification of Target Placement for COS at LP5" (PID 16430, PI E. Frazer) was designed to observe the white dwarf standard star WD0947+857, scanning the target across the aperture in order to measure the throughput as a function of target position. The observations consisted of one two-orbit visit that placed the G130M/1291 FP-POS=3 spectrum of WD0947+857 at the fiducial lifetime position, which lies approximately +5.4" above LP1 or 10.4″ above LP4, and took a series of exposures, each with an exposure time of 21 seconds, while moving the target across the fixed primary science aperture (PSA) in both the dispersion and cross-dispersion directions. The dispersion and cross-dispersion scans are each in their own Non-Interruptible Sequence in separate orbits in order to complete the scan as quickly as possible without interruptions. In this work, we denote the along-dispersion

direction scan as the X scan, and the cross-dispersion scan as the Y scan.

We adopted a pattern of POS TARG offsets in arcseconds relative to the nominal target center of: -1.38, -1.10, -0.86, -0.67, -0.48, -0.29, -0.14, 0.00, +0.14, +0.29, +0.48, +0.67, +0.86, +1.10, +1.38 in both the X and Y directions independently. This pattern was chosen to mimic the observation strategy that was used for PID 14875 ("Verification of Aperture and FUV Spectrum Placement for COS at LP4," PI D. Sahnow, see COS ISR 2018-17), which performed the same function for LP4. That program held the target position fixed and scanned the aperture with X and Y shifts of -29, -23, -18, -14, -10, -6, -3, 0, +3, +6, +10, +14, +18, +23, +29 steps. We used the plate scale conversion of 21 steps per arcsecond (COS ISR 2018-17) to calculate the equivalent POS TARG offsets for this program. We cannot use the same method as the LP4 program because of the light leak that occurs when the wavecal lamp is turned on and the aperture block is commanded to LAPXSTP$<$12. At LP5, the aperture block is fixed at a safe position just below where the light leak will occur so that wavecals can be performed (and though we take them in this program, we do not use them for the analysis). An advantage to scanning the target is that it can be moved in finer steps than the aperture block, which we did not employ in our case, but could be useful for future programs. Other changes from the LP4 program included the use of G130M/1291 instead of G130M/1309 in order to use both segments per the COS2025 rules, as well as changing the target from WD0308-565 for better schedulability.

The visit was initially executed on October 19, 2020, but failed due to a guide star lock issue which caused all exposures to have an exposure time of zero seconds. The repeat observations were completed on November 9, 2020. Table 1 lists the exposures for both scans, along with their right ascension (RA) and declination (Dec), angular separation from the center of the scan (same as the POSTARG offset), and relative count level for both detector segments. Figure 1 shows a visual representation of the FUVA exposures in this program, plotted as circles in RA and Dec on the sky. The color of each circle represents the number of counts in each exposure. As expected, the counts increase toward the center of each scan.

3. Calibration

The data in PID 16430 were set in the Astronomer's Proposal Tool (APT) to bypass calibration in the Barbara A. Mikulski Archive for Space Telescopes (MAST) archive, since reference files for LP5 were not available in the Calibration Reference Data System (CRDS) at the time. This configuration also prevents users from using these observations for scientific purposes. Therefore we start with `rawtag` files for the exposures, and manually calibrate them using the `CalCOS` pipeline. We changed the following keywords in the `rawtag` headers to "OMIT": FLATCORR, X1DCORR, WAVECORR, FLUXCORR, and TDSCORR. We also set the RANDSEED value to "123456789" for all exposures so that the positions of the events are all randomized in the same way. We process these updated files through `CalCOS` version 3.3.10 to

Table 1. The exposures taken in PID 16430, listed in order of their observation. The first column gives the observation number, which corresponds to the numbers printed in Figure 1. The second column gives the rootname. The third column denotes whether the exposure is a part of the X or Y scans. The fourth and fifth columns give the center RA and Dec of the target in the aperture. The sixth column lists the time of the observation. The seventh and eighth columns give the relative counts for the FUVA and FUVB detectors, respectively. The ninth column gives the angular separation in arcseconds from the center position of the scan to the coordinates of the exposure calculated from the RA and Dec, which equals the POSTARG offset applied in APT.

Obs. #	Rootname	Scan	RA	Dec	Obs. Time	FUVA Counts	FUVB Counts	Sep (″)
0	legy51a7q	Y	149.4749	85.4945	00:28:05	0.993	0.996	-0.00
1	legy51aaq	Y	149.4773	85.4941	00:30:08	0.276	0.263	-1.38
2	legy51acq	Y	149.4768	85.4942	00:32:11	0.605	0.604	-1.10
3	legy51aeq	Y	149.4764	85.4943	00:34:14	0.767	0.764	-0.86
4	legy51agq	Y	149.4761	85.4943	00:36:17	0.871	0.874	-0.67
5	legy51aiq	Y	149.4757	85.4944	00:38:20	0.959	0.959	-0.48
6	legy51akq	Y	149.4754	85.4944	00:40:23	0.990	0.979	-0.29
7	legy51amq	Y	149.4752	85.4944	00:42:26	0.993	0.992	-0.14
8	legy51aoq	Y	149.4749	85.4945	00:44:29	0.993	0.992	-0.00
9	legy51aqq	Y	149.4747	85.4945	00:46:32	0.995	0.984	0.14
10	legy51asq	Y	149.4744	85.4946	00:48:35	0.983	0.972	0.29
11	legy51auq	Y	149.4741	85.4946	00:50:38	0.914	0.897	0.48
12	legy51awq	Y	149.4738	85.4946	00:52:41	0.825	0.805	0.67
13	legy51ayq	Y	149.4735	85.4947	00:54:44	0.711	0.690	0.86
14	legy51b0q	Y	149.4731	85.4948	00:56:47	0.516	0.486	1.10
15	legy51b2q	Y	149.4726	85.4948	00:58:50	0.208	0.185	1.38
16	legy51b4q	Y	149.4749	85.4945	01:00:53	1.000	1.000	0.00
17	legy51bgq	X	149.4749	85.4945	01:56:20	0.993	1.000	-0.00
18	legy51biq	X	149.4706	85.4943	01:58:23	0.321	0.328	-1.38
19	legy51bkq	X	149.4715	85.4943	02:00:26	0.624	0.627	-1.10
20	legy51bmq	X	149.4723	85.4944	02:02:29	0.780	0.784	-0.86
21	legy51boq	X	149.4728	85.4944	02:04:32	0.867	0.880	-0.67
22	legy51bqq	X	149.4734	85.4944	02:06:35	0.967	0.960	-0.48
23	legy51bsq	X	149.4740	85.4944	02:08:38	0.997	0.985	-0.29
24	legy51buq	X	149.4745	85.4945	02:10:41	0.995	0.999	-0.14
25	legy51bwq	X	149.4749	85.4945	02:12:44	0.996	0.998	-0.00
26	legy51byq	X	149.4754	85.4945	02:14:47	0.993	0.992	0.14
27	legy51c0q	X	149.4758	85.4945	02:16:50	0.990	0.980	0.29
28	legy51c2q	X	149.4764	85.4945	02:18:53	0.909	0.906	0.48
29	legy51c4q	X	149.4770	85.4946	02:20:56	0.825	0.821	0.67
30	legy51c6q	X	149.4776	85.4946	02:22:59	0.734	0.729	0.86
31	legy51c8q	X	149.4783	85.4946	02:25:02	0.556	0.547	1.10
32	legy51caq	X	149.4792	85.4947	02:27:05	0.254	0.250	1.38
33	legy51ccq	X	149.4749	85.4945	02:29:08	1.000	0.999	0.00

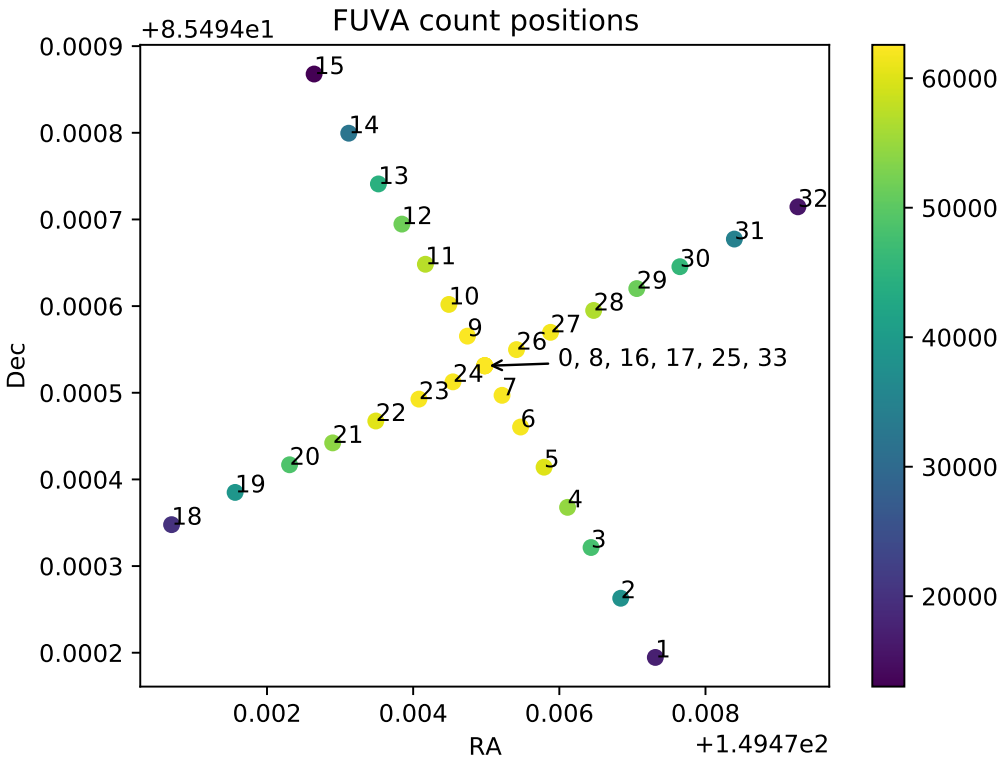

Figure 1. The coordinates of the center of the PSA in PID 16430, plotted as circles in RA and Dec in degrees. The color of each circle represents the number of counts in each exposure, which are enumerated in the colorbar on the right. The numbers for each point correspond the the exposure number listed in Table 1.

produce temperature and walk-corrected `corrtag` files that we use for the remainder of this analysis.

4. Analysis

We first create 2 dimensional images for every exposure using the XCORR and YCORR arrays in the `corrtag` files. Each event in each file is binned to make images for both segments separately. The plots in Figure 2 show examples of these images for both FUVA (top) and FUVB (bottom). We then sum the counts in every image inside a pre-defined rectangular region; the red rectangles in Figure 2 show where these lie. For FUVB, we exclude the Ly-α airglow region (XCORR$\sim$9100) from the total counts. Next, we compute the relative counts in each exposure and segment by dividing each sum by the exposure with largest sum of counts. We do this for each scan separately. We lastly compute the separations of each exposure, relative to the scan center, using the RA and Dec coordinates of the center of the aperture. These separations are the same as the POSTARG values we employed in APT. These values for every observation are given in the last three columns of Table 1.

With these data, we can compare the relative counts versus POSTARG offset for both segments, as shown in the throughput curves in Figure 3. The X (along dispersion) scan is shown on the top, and the Y (cross dispersion) scan is on the bottom. In both plots, FUVA is represented by pink circles, while FUVB is represented by blue crosses. We compute the best center value for several different percentages of the throughput along the curve. These are shown by the pink and blue dashed horizontal lines that span 30% (Y scan only), 40%, 50%, 60%, 70%, 80%, 90%, 95%, and 97.5% throughput. The best centers and the left and and right intercepts of the throughput curve for each level is marked with a star (pink for FUVA and blue for FUVB). We then compute the median of all center values (combining measurements from both segments) to find the final adjustment in arcseconds needed for each scan direction, which is shown by the black vertical line in each plot. We calculate -0.0454″ for the X scan, and -0.0492″ for the Y scan.

In Figure 4, we alternatively show this same best center data, as a function of the half width at various throughput levels, for the X scan (top) and Y scan (bottom). The half widths are half of the distances between where each throughput level intersects the throughput curve on either side of the scan (i.e., half of lengths of the dashed horizontal lines in Figure 3). Again, the FUVA data are shown in pink crosses, and FUVB is shown in blue. The final offset is also plotted as the black horizontal line. Visualization in this manner helps determine if the median offset is a good representation of the entire throughput curve. For both scans, we see that as the half width increases, the best center trends toward 0″ offset. The exception is the smallest half width (which represents the 97.5% throughput data point), where the best center moves more toward zero again. We believe this systematic shift is due to a slight asymmetry of the COS point spread function at the aperture. The overall scatter observed in the plots falls well within the

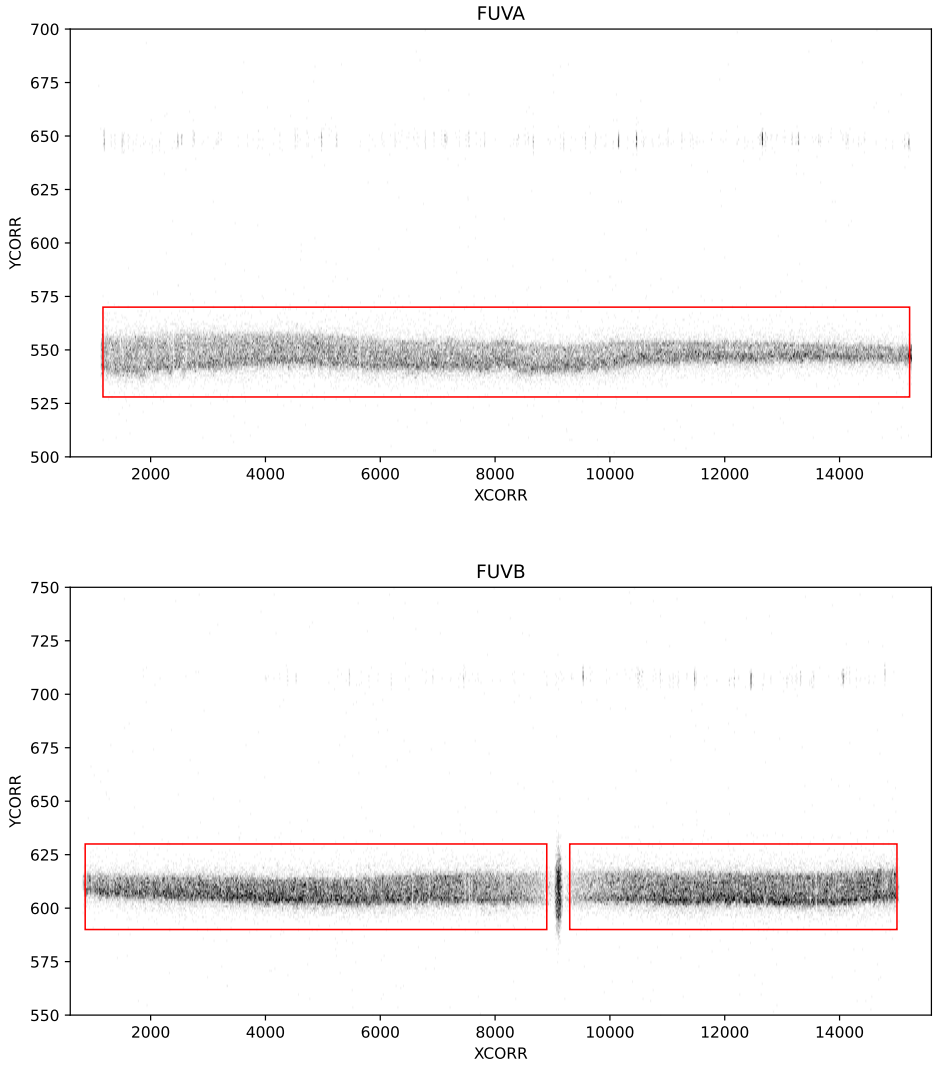

Figure 2. Example two dimensional images of a `corrtag` file for FUVA (top) and FUVB (bottom) in XCORR and YCORR units for one of the exposures in the target placement program. The red rectangles show the regions where counts are summed for this analysis. We exclude the wavelength calibration spectrum for both segments and the Ly-α airglow region for FUVB.

COS/FUV/G130M target acquisition centering requirements of $\pm 0.106''$ in the along dispersion direction and $\pm 0.3''$ in the cross dispersion direction (COS ISR 2023-01), so we conclude that the median offset well-represents all data for both segments in each scan.

5. Final SIAF Adjustments

To update the SIAF, we must first convert the X and Y offsets found in our analysis in the COS coordinate plane into the telescope's focal plane coordinates, V2 and V3. A visualization showing COS's detectors in relation to the HST focal plane is shown on the left side of Figure 5. This figure and more information about the SIAF can be found on the HST Aperture Resources page on the STScI website. COS is rotated by roughly 45°with respect to the (V2, V3) coordinate system, allowing for simple trigonometric conversions of the offsets. We find the V2 and V3 projections of the measured X and Y offsets using the equations:

$$
\begin{aligned}
V2_X &= \sin(45^\circ) \times -0.0454'' \\
V3_X &= -\cos(45^\circ) \times -0.0454'' \\
V2_Y &= \sin(45^\circ) \times -0.0492'' \\
V3_Y &= \cos(45^\circ) \times -0.0492''
\end{aligned}
$$

Note that $V3_X$ is negative because positive V3 is pointing downwards. The right panel in Figure 5 shows a sketch of the two coordinate systems superimposed, where the vectors of our calculated X and Y offsets are denoted with pink arrows. Then to find the final offsets we add:

$$
\begin{aligned}
V2 &= V2_X + V2_Y = -0.06690'' \\
V3 &= V3_X + V3_Y = -0.00266''
\end{aligned}
$$

The above V2 and V3 offsets are lastly added to the initial values for the LFPSA5, LFBOA5, LAPTFPSA5, and LAPTFBOA5 in the SIAF to calculate the final values that are used to update the file. Table 2 lists the initial and updated values for all aperture positions.

6. Summary

The best target placement for observations through the PSA at LP5 was determined through an analysis of throughput as a function of target position in the along dispersion (X) and cross dispersion (Y) directions. We determined that the optimal target position required X and Y offsets of -0.0454" and -0.0492", respectively, relative to the nominal

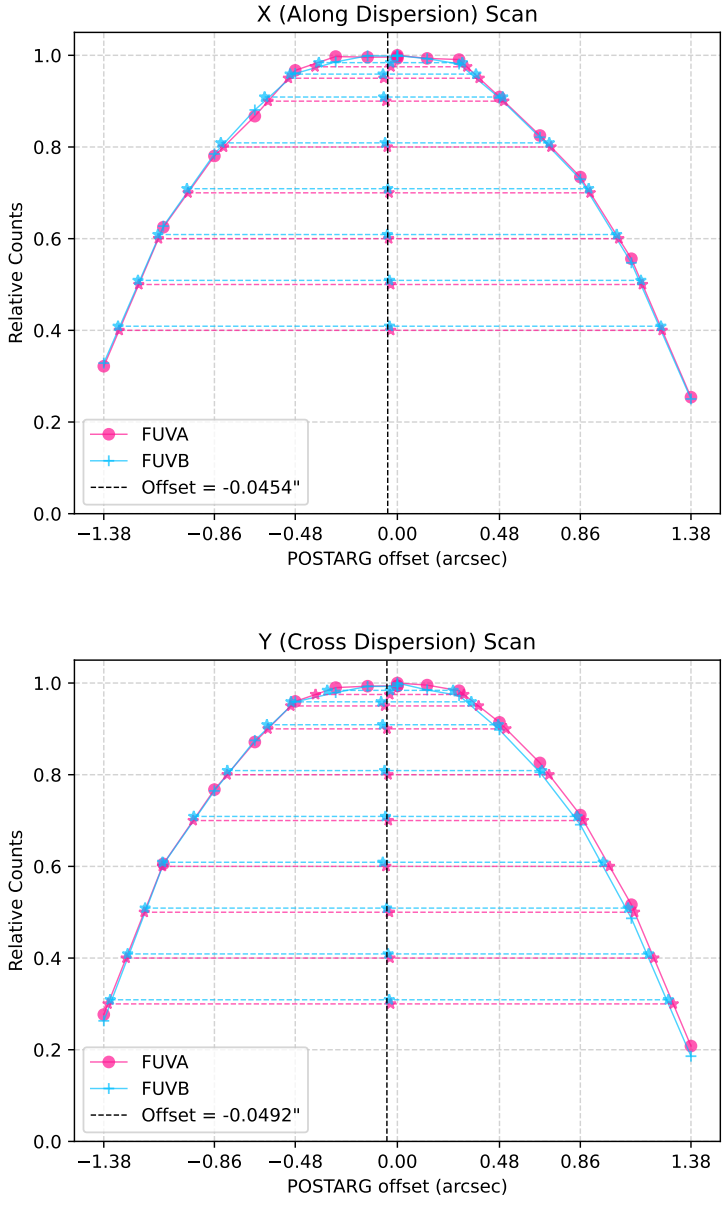

Figure 3. Relative counts versus POSTARG offset (in arcseconds) for both the X scan (top) and Y scan (bottom). FUVA data is represented by pink circles, while FUVB is represented by blue crosses. The horizontal lines show where 30% (Y scan only), 40%, 50%, 60%, 70%, 80%, 90%, 95%, and 97.5% of the maximum throughput for each segment lie. We compute the best centers for each percentage throughput (central pink or blue stars), and then find the median offset of these values to determine the final shift for each scan (denoted by the black vertical line).

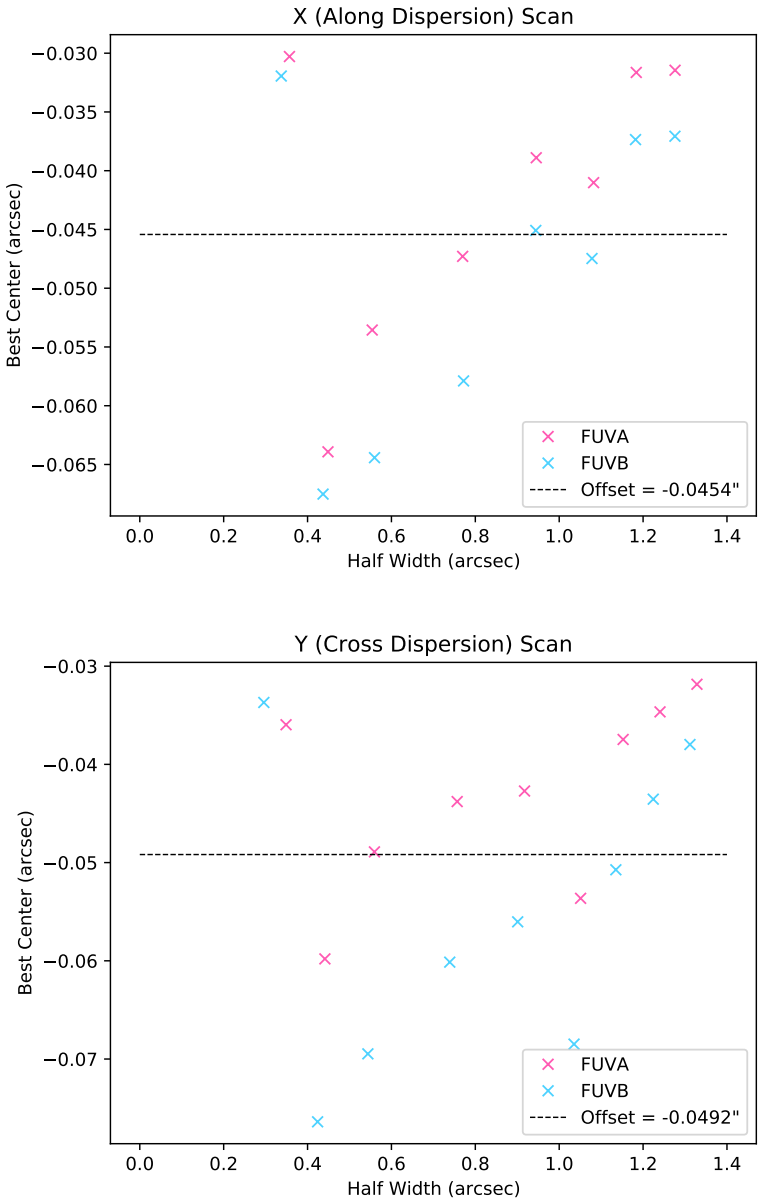

Figure 4. Best center (in arcseconds) versus half width (in arcseconds) for the X scan (top) and Y scan (bottom). The FUVA data are shown in pink, and FUVB in blue. The black dotted line shows the final offset calculated for each scan.

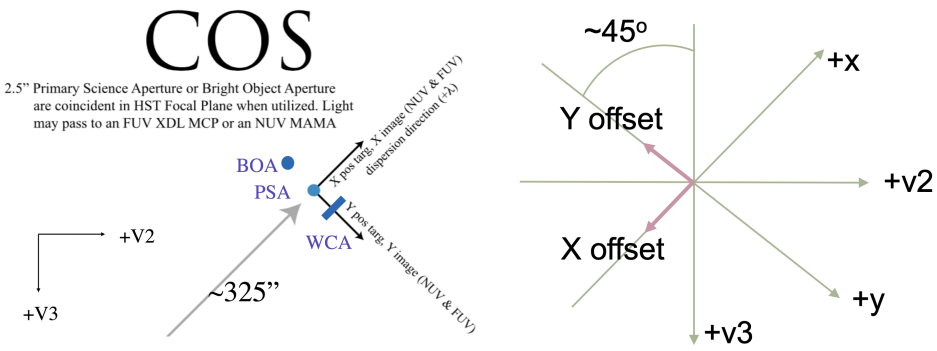

Figure 5. Left: The COS X, Y coordinates in relation to the HST focal plane coordinate V2, V3. The two coordinate systems are rotated by 45°. This figure and more information can be found on the HST Aperture Resources page on the STScI website. Right: Simplified sketch showing the two coordinate systems overlaid, with the pink arrows denoting the directions of X and Y offsets calculated in this analysis.

Aperture	Nominal V2	Nominal V3	Updated V2	Updated V3
LFBOA5	236.5414	-233.6966	236.4745	-233.6993
LFPSA5	236.5414	-233.6966	236.4745	-233.6993
LAPTFBOA5	227.1672	-243.0708	227.1003	-243.0735
LAPTFPSA5	245.9156	-224.3224	245.8487	-224.3251

Table 2. Nominal and Adopted LP5 SIAF values

pointing. These correspond to V2 and V3 offsets of -0.06690" and 0.00266". The adjustments were made in the SIAF in February 2021 as a FSW patch, and later in September installed permanently, for all LP5 data to use.

Change History for COS ISR 2025-05

Version 1: 1 April 2025- Original Document

References

James et al. 2023, COS Instrument Science Report 2023-10
Penton, S. & Sahnow, D. 2023, COS Instrument Science Report 2023-01
Sahnow, D. & Penton, S. 2018, COS Instrument Science Report 2018-17
Sankrit, R., et al. 2023, COS Instrument Science Report 2023-25